

Micro-Scale Homogenization of Fiber Composites Using an Automated Graphical User Interface Based Python Abaqus Interface

Nguyen Duc Hai*

Faculty of Mechanical and Automotive Engineering, Thanh Dong University, Hai Phong, Vietnam

*Corresponding author email: nguyenduchai@hnu.edu.cn

Abstract

This study introduces the Micro-scale RVE Tool (MRT) and Quick Tool Model (QTM) for efficient prediction of the effective elastic properties of composite materials. A Python-based interface enables streamlined meshing, modeling, and property extraction. Compared to conventional methods, the approach significantly reduces computation time by optimizing code structure and automating stiffness parameter extraction. The MRT is built on multi-scale homogenization theory and allows for three-dimensional representative volume element (RVE) generation with varied fiber geometries. Finite element (FE) analysis and volumetric homogenization are used to compute elastic properties across different fiber volume fractions. Results show strong agreement with experimental data, validating the accuracy and efficiency of the proposed method. Notably, parametric studies reveal that fiber eccentricity and rotation angle (0° to 150°) significantly affect transverse moduli and Poisson's ratios, while longitudinal stiffness remains stable. The QTM enables rapid property estimation without full FE simulations, reducing computational cost by over 70%. Validated against T300/Epoxy and Boron/Aluminum composites, deviations are below 5% for longitudinal modulus. This open-source, user-friendly framework provides a robust foundation for multi-scale design and optimization of advanced composites in aerospace, automotive, and marine applications. In summary, this study offers a practical, time-saving alternative to conventional homogenization methods.

Keywords: Constitutive modeling, composite structure, homogenization, micro-scale, RVE, structural analysis.

1. Introduction

Composite materials consist of two or more distinct phases, typically a continuous matrix and a dispersed reinforcement such as fibers, combined to achieve superior mechanical properties compared to traditional monolithic materials [1]. The matrix transfers load and binds the structure, while the reinforcement provides strength and stiffness. In recent years, growing interest has been directed toward the use of natural fillers in polymer composites due to their potential to enhance mechanical behavior while supporting environmental sustainability. Derived from renewable sources, these fillers reduce production cost and carbon footprint, and offer benefits such as improved damping, impact resistance, and thermal insulation.

Fiber-reinforced polymer (FRP) composites are increasingly employed in aerospace, marine, biomedical, and civil engineering applications due to their outstanding impact resistance, abrasion resistance, and superior strength-to-weight ratio. However, the inherent heterogeneity of their microstructure and the complexity of manufacturing processes often lead to multi-scale damage, complicating accurate mechanical characterization. While experimental techniques remain the benchmark for material evaluation, they are often time-consuming, expensive, and limited in their

scalability [1]. As an efficient alternative, multi-scale modeling based on finite element analysis (FEA) and Representative Volume Elements (RVEs) has been widely adopted to predict effective elastic properties by bridging microstructural features to macro-level behavior [2].

Polymer matrix composites are typically manufactured using thermoplastics or thermosets combined with synthetic or natural fibers. Common production methods include injection molding, compression molding, resin transfer molding, and filament winding. These processes significantly affect fiber orientation, distribution, and interfacial quality factors that influence the microstructure and consequently, the effective mechanical properties.

Polymer-based composites, especially fiber-reinforced polymers (FRPs), are widely used in industries due to their high strength-to-weight ratio, corrosion resistance, and design flexibility. These advantages contribute to fuel efficiency in transportation and longer durability in harsh environments. However, limitations such as low bearing capacity under localized loads and susceptibility to wear or matrix cracking remain challenges, particularly at the fiber-matrix interface. FRPs are applied across various sectors including

aerospace, automotive, shipbuilding, and biomedical where weight reduction and performance are critical. While carbon fiber reinforced polymer (CFRP) is preferred in aircraft structures for its high stiffness, Glass Fiber Reinforced Polymer (GFRP) is commonly used in marine applications due to its lower cost and good damping behavior.

This paper proposes an open-source, Python-based tool integrated with Abaqus Computer-Aided Engineering (CAE) for automated generation, meshing, and periodic boundary condition (PBC) application in 3D FRP RVE models. Unlike existing methods that often require manual setup or assume idealized microstructures, the tool supports irregular fiber arrangements, eccentric positions, and random geometry variations that better reflect manufacturing realities. The main contribution lies in the combination of computational efficiency, user accessibility via Graphical User Interface (GUI), and realistic RVE modeling. This research addresses the lack of practical, user-friendly tools for accurate micro-scale property prediction, and offers a reproducible, flexible solution for both academic and industrial composite design workflows.

Numerous studies have demonstrated the potential of RVE-based modeling to capture deformation mechanisms and interfacial effects in composites. For example, Li *et al.* [3] addressed pressure sensitivity and isotropic damage in epoxy matrices, while Chu *et al.* [4] implemented Periodic Boundary Conditions (PBCs) to predict elastic properties in composites containing random voids. Liu *et al.* [5] explored failure mechanisms in glass fiber composites using explicit Finite Element (FE) Representative Volume Element (RVE) simulations. However, many existing models assume periodic or idealized fiber distributions, which do not account for manufacturing-induced imperfections such as misalignment, irregular spacing, or fiber deformation. These imperfections introduce stochastic effects that can significantly affect local stress distributions and global mechanical responses [6, 7], yet they remain underrepresented in practical tools for micro-scale modeling.

Although analytical and numerical homogenization methods have been proposed to estimate composite properties [8, 9], periodic fiber arrangements fail to capture key heterogeneities, especially in transverse deformation, as shown by Brockenbrough *et al.* [10]. Recent advances, including fiber randomization techniques [11] and image-based microstructure reconstruction using nearest-neighbor algorithms (e.g., Vaughan and McCarthy [12]), offer greater realism but often require specialized equipment and are computationally intensive [13]. Therefore, there remains a critical need for robust, efficient, and user-friendly tools capable of simulating realistic RVEs with random fiber distributions and imperfections.

To address these gaps, this study presents a finite element-based computational framework to evaluate the elastic properties of composite materials at the micro-scale using 3D periodic RVEs. A Python-powered tool Micro-scale RVE Tool (MRT) is developed and integrated into the Abaqus CAE environment. This tool enables automated application of periodic boundary conditions, intuitive mesh control, and efficient data extraction via a graphical user interface. The MRT supports the generation of RVEs with realistic geometric variability, such as eccentric or randomly placed fibers, thereby reflecting actual manufacturing conditions. Simulation results are validated against experimental data and prior numerical models, demonstrating the tool's effectiveness in capturing key stochastic effects and supporting accurate multi-scale design and failure analysis of fiber-reinforced composites.

2. Homogenization and Modeling Method

The RVE homogenization method estimates effective elastic properties by applying uniform deformation to periodic microstructures, with accuracy dependent on proper enforcement of PBCs [14]. Unlike simplified models such as Chamis [15], FE-based approaches account for geometric variability and complex nonlinear behaviors [16]. Flat boundary assumptions can cause significant errors in orthotropic and shear predictions [17, 18]. To address this, the MRT was developed in Abaqus to automate PBC implementation and property extraction via constraint equations and displacement fields [19]. Results align well with experimental data [20], with slight deviations due to mesh sensitivity. The tool's Python interface and GUI enable intuitive control of fiber geometry and mesh generation, offering reliable predictions of mechanical behavior even with non-stochastic, yet geometrically varied fiber distributions are illustrated in Fig. 1.

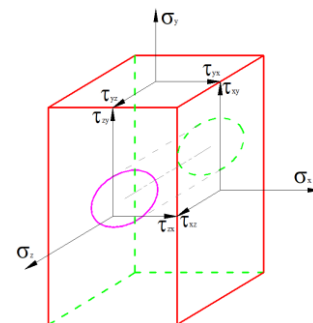
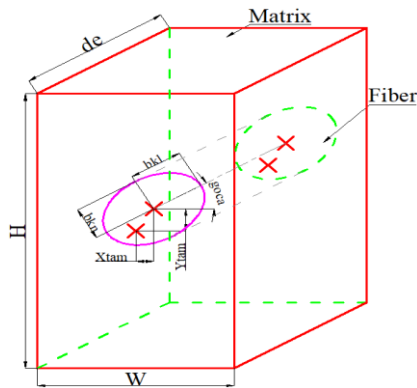
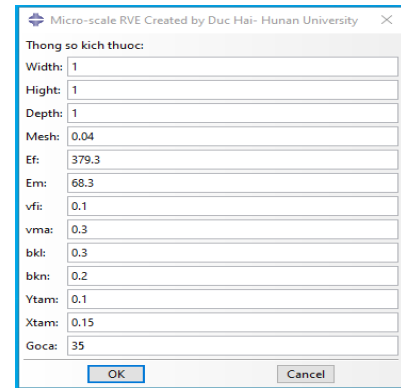


Fig. 1. Schematic representation of displacement boundary conditions required to estimate the effective elastic properties

The basic square and hexagonal arrangements of fiber-matrix composites are illustrated in Fig. 2, respectively, representing common configurations in micro-scale RVE studies.



(a) Square unit cell with centered fiber



(b) Hexagonal unit cell with centered fiber

Fig. 2. Geometry of single-fiber RVE configurations with fiber-matrix interface

In continuous fiber-reinforced composites, fiber length is typically aligned with the product length, satisfying periodic boundary conditions. However, in practice, fiber cross-sections are randomly distributed and may deform under manufacturing-induced compression. Among various RVE configurations, square and hexagonal fiber arrangements are widely accepted as representative of real microstructures. Therefore, this study employs square and hexagonal periodic RVEs to investigate the effective properties of fiber-reinforced composites under different geometric scenarios.

The square and hexagonal fiber arrangements used in this study are shown in Fig. 3, representing representative microstructural configurations commonly adopted in RVE modeling.

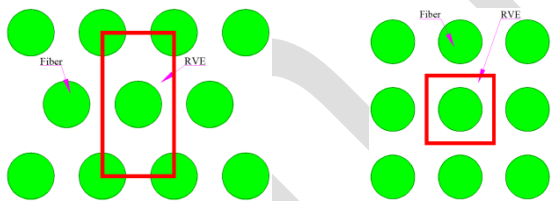


Fig. 3. Square and hexagonal arrangement of fibers

Numerous methods exist for generating RVEs with random fiber distributions, but these often involve high fiber counts, leading to large meshes and significant computational costs. This study introduces an efficient 3D micro-scale modeling approach that enables flexible control over fiber position, size, and eccentricity-effectively capturing random distributions while minimizing computational demand. The process is automated via Python and executed within Abaqus through a custom GUI, requiring only basic material inputs. RVE generation completes in 6–8 seconds, and mesh sensitivity analysis confirms reliable predictions even at low mesh densities. The tool streamlines simulation setup and directly extracts effective elastic properties, offering a fast, accurate, and user-friendly

framework for multi-scale composite analysis. The overall workflow for the automated RVE generation, meshing, application of periodic boundary conditions, and extraction of effective elastic properties is summarized in Fig. 4.

The process begins with defining RVE dimensions, material properties, and mesh size via a user-friendly GUI. These inputs are transferred to Abaqus, where nodal coordinates define RVE boundaries and serve to construct geometry and identify surfaces for simulation. Node sets are automatically generated to apply PBCs, ensuring mesh continuity across opposing faces. If meshing fails, the tool prompts re-meshing through the GUI.

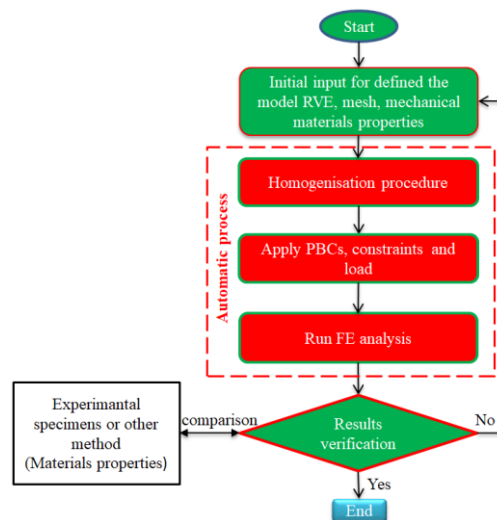


Fig. 4. Flow chart of algorithm method predicting RVE mechanical properties

Mesh density influences accuracy, but beyond a threshold, improvements become negligible while increasing computational cost. Elastic properties are predicted using constraint equations that impose PBCs and displacement conditions. Each elastic constant is computed individually: effective stress is obtained from

boundary nodal forces, and Young's modulus is calculated as the stress-to-strain ratio. Poisson's ratio and shear modulus are similarly derived from reaction forces and corresponding deformations, ensuring accurate estimation of effective elastic behavior.

3. Materials and Periodic Boundary Conditions

3.1. Materials

In this study, the reinforcement content is defined in terms of Fiber Volume Fraction (V_f), as it directly governs the spatial distribution of fibers and the effective mechanical response in RVE-based micromechanical modeling.

Continuous fiber-reinforced composites are heterogeneous two-phase materials in which load-bearing fibers are bonded by a surrounding matrix. This study examines two prototypical RVE geometries, namely square and hexagonal, which have been validated in prior work. Effective properties (Table 1 and Table 2) were computed using a 3D FE model in Abaqus with C3D8R elements, mesh sizes set via convergence studies. Rather than manual homogenization, we introduce a Python based RVE GUI tool that automates RVE construction, PBC application (accounting for non planar deformations), and elastic property extraction. The open source tool delivers FEA level accuracy in far fewer iterations and drastically reduced computation time.

Table 1. The mechanical properties of Carbon T300/Epoxy materials [21]

Material	Fiber	Matrix
Young's modulus (GPa)	230	3.12
Poisson's ratio	0.26	0.38

Table 2. The mechanical properties of boron/aluminium materials [22]

Material	Fiber	Matrix
Young's modulus (GPa)	379.3	68.3
Poisson's ratio	0.1	0.3

3.2. Periodic Boundary Conditions

Three-dimensional PBCs are applied to the RVE to ensure periodicity of the stress and strain fields. These conditions are enforced by prescribing nodal displacements along the RVE boundaries such that both displacement and traction continuity are satisfied across opposing faces. The PBCs are defined by the relative displacement relationships between corresponding nodes on opposite boundary surfaces, as expressed in the following formulation:

$$u_i^{j+}(x, y, z) - u_i^{j-}(x, y, z) = c_i^j (i, j = 1, 2, 3) \quad (1)$$

The constants c_1^1, c_2^2 and c_3^3 represent the average elongation or contraction of the RVE model due to the action of the three normal tensile force components, while the remaining three pairs of constants $c_1^2 = c_2^1, c_1^3 = c_3^1$, and $c_2^3 = c_3^2$ correspond to the shear strains due to the three shear force component. Based on homogenization theory, effective stress and strain calculations for RVE are performed by spatially averaging the microscopic responses. The average stress and strain in RVE are defined according to the following formula:

$$\bar{\varepsilon}_{ij} = \frac{1}{V} \int_V \varepsilon_{ij} dV \quad (2)$$

$$\bar{\sigma}_{ij} = \frac{1}{V} \int_V \sigma_{ij} dV \quad (3)$$

where V is the volume of the representative periodic volume element. The macroscopic strain is calculated as follows:

$$\varepsilon_{ij} = \frac{U_i}{L_j} \quad (i \neq j) \quad (4)$$

Macroscopic stress is expressed as follows:

$$\varepsilon_{ij} = \frac{\Delta x_j}{V} \int_{S_j} \sigma_{ij} dS = \frac{P_{ij}}{S_j} \quad (i \neq j) \quad (5)$$

where S_j is the area of j^{th} the boundary surface on which the displacement is applied, P_{ij} is the tensile force on the load-bearing surface. The average stress can be obtained from the tensile force results on the boundary surfaces by dividing them by the area of the corresponding boundary surfaces.

The RVE 3D FE micro-scale material models are meshed as C3D8R, periodic boundary conditions are imposed on the microstructures to create constant strain and stress compatibility, which can be expressed as displayed as follows:

$$\begin{aligned} U(W_x, y, z) - U(0, y, z) &= U_1 \\ U(x, H_y, z) - U(x, 0, z) &= U_2 \\ U(x, y, De_z) - U(x, y, 0) &= U_3 \end{aligned} \quad (6)$$

where $U(x, y, z)$ is the displacement vector at point (x, y, z) . W_x, H_y and De_z are the dimensions of the RVE in x, y and z directions, respectively.

Six distinct loading conditions-longitudinal tension, transverse tension, and longitudinal shear are applied to the micro-scale RVE, as illustrated in Fig. 1. According to Hill [23], the volume average of a quantity is defined as the integral of that quantity over the RVE volume divided by the total volume. Thus, the volume-averaged stress for the RVE is expressed as:

$$\bar{\sigma}_{ij} = \frac{1}{V} \int_V \sigma_{ij} dV \quad (7)$$

$$\bar{\varepsilon}_{ij} = \frac{1}{V} \int_V \varepsilon_{ij} dV \quad (8)$$

The elastic constants of the mixture according to Young's modulus, Poisson's ratio and shear modulus can be calculated from the macroscopic stress and strain tensor as follows:

$$E_{ii} = \frac{\bar{\sigma}_{ii}}{\bar{\varepsilon}_{ii}}, \quad \nu_{ij} = -\frac{\bar{\varepsilon}_{ij}}{\bar{\varepsilon}_{ii}}, \quad G_{ij} = \frac{\bar{\tau}_{ij}}{\bar{\gamma}_{ij}} \quad (9)$$

4. Results and Discussion

The proposed micro-scale RVE model aims to efficiently predict the effective elastic properties of composites based on constituent phases. FEA combined with volumetric homogenization is used under six independent loading conditions to extract the stiffness tensor. Results show at Table 3 and Table 4 align closely with experimental data and prior studies, validating model accuracy. The stress distributions corresponding to the six independent loading conditions for the hexagonal RVE configuration are illustrated in Fig. 5 and Fig. 6.

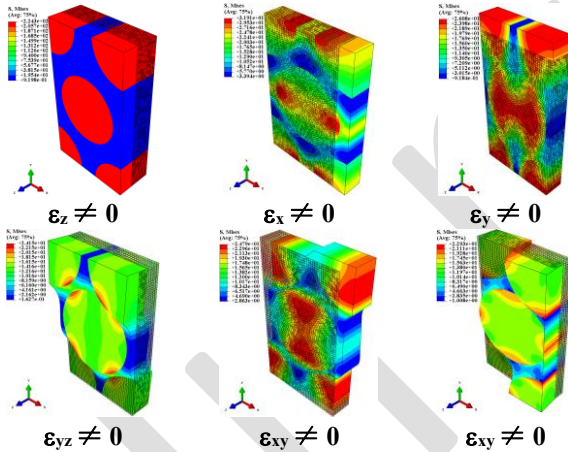


Fig. 5. Stress state of micro-scale RVE hexagonal arrangement with six independent states

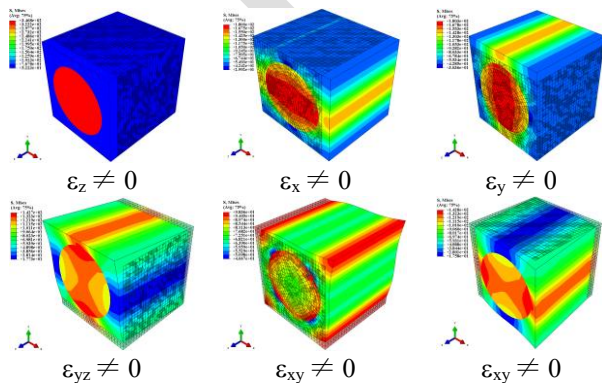


Fig. 6. Stress state of micro-scale RVE square arrangement with six independent states

Fiber stiffness primarily governs the longitudinal modulus E_1 , while the matrix influences transverse properties. Despite a constant fiber volume fraction, the model captures property variations due to constituent differences. The Python-based, Abaqus-integrated tool supports rapid, automated simulations, customizable fiber geometries, and multi-phase configurations.

Table 3. Results and comparison for unidirectional Carbon T300/Epoxy ($V_f = 0.752$)

Material parameter	Present	Luciano and Barbero, 1994
E_1	173.66	173.864
E_2	24.3	22.135
E_3	24.3	22.135
G_{12}	7.386	8.611
G_{13}	8.71	-
G_{23}	8.708	7.796
ν_{12}	0.2846	0.278
ν_{13}	0.3956	-
ν_{23}	0.3957	0.42

Table 4. Results and comparison for unidirectional Boron/aluminum ($V_f = 0.47$)

Material parameter	Present	Ref 13
E_1	215	214
E_2	143.75	143
E_3	143.75	143
G_{12}	54.16	54.2
G_{13}	57.25	-
G_{23}	57.25	45.7
ν_{12}	0.194	0.195
ν_{13}	0.255	-
ν_{23}	0.255	0.253

The predicted effective elastic constants for both Carbon/Epoxy and Boron/Aluminum composites show strong agreement with reference data from Luciano and Barbero [21] and Ye *et al.* [22], with deviations typically within 5–10%. For instance, the predicted longitudinal modulus $E_1 = 173.66$ GPa for T300/Epoxy ($V_f = 0.752$) closely matches the experimental value of 173.86 GPa [21]. Slight variations in transverse properties are attributed to the inclusion of fiber misalignment and geometric variability in our model, which are often neglected in idealized RVE formulations. This demonstrates the capability of our model to better reflect manufacturing imperfections and provides improved realism over conventional methods that assume perfectly periodic fiber distributions.

Fibers are modeled as transversely isotropic. Elastic constants are derived from reaction forces at RVE boundaries. As expected, transverse strengths are lower than longitudinal ones, consistent with experimental observations. The framework offers reliable, efficient microscale characterization of composite materials.

4.1. Effect of Random Fiber Size

Manufacturing factors can cause random fiber diameter variations, leading to elliptical deformation in the RVE. To assess their impact, models with constant V_f but varying fiber diameters (0%, ±5%, ±10%, ±15%) are analyzed. The RVE types hexagonal ($V_f = 0.752$) is used to study the effect of fiber shape distortion on effective mechanical properties. The variation in effective moduli under different levels of fiber diameter distortion is presented in Fig. 7 for T300/Epoxy.

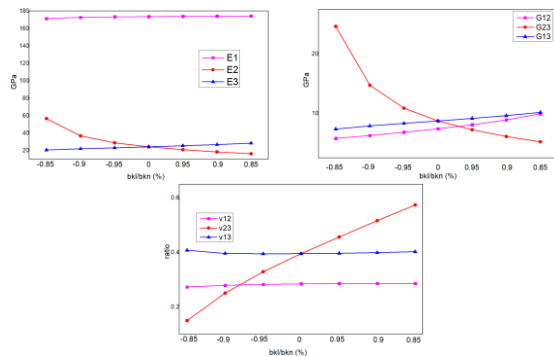


Fig. 7. Effect of fiber diameter variation on the effective mechanical properties of composites

Results indicate that fiber diameter randomness has minimal impact on longitudinal Young's modulus (E_1). However, incorporating deformed fiber interfaces is a critical step toward accurately evaluating the effective properties of complex composites.

4.2. Affects Representative Volume Elements Interface

Building on the verified accuracy of the proposed model, this section examines the effect of fiber position deviations from ideal locations. Simulations were conducted with a fiber volume fraction of V_f equal 0.2, using eight eccentric fiber positions defined by normalized coordinates (Y_{center}/R , X_{center}/R). These variations reflect practical manufacturing imperfections in fiber alignment, which influence local stress distributions and composite performance. To evaluate this, 144 RVEs with varied fiber diameters were generated under both square and hexagonal configurations. Fiber eccentricity was used as a simplified representation of randomness. FEM simulations revealed that the longitudinal modulus E_1 remains largely unaffected by eccentricity, while transverse moduli and Poisson's ratios exhibit significant variations. This indicates that eccentric RVEs capture more realistic stress-strain behavior compared to ideal central-fiber models.

Fig. 8 show the sensitivity of elastic properties to fiber misalignment in both materials. Results underscore the importance of incorporating fiber misalignment in RVE modeling to better represent actual composite microstructures, particularly for

predicting transverse properties sensitive to fiber-matrix interface conditions.

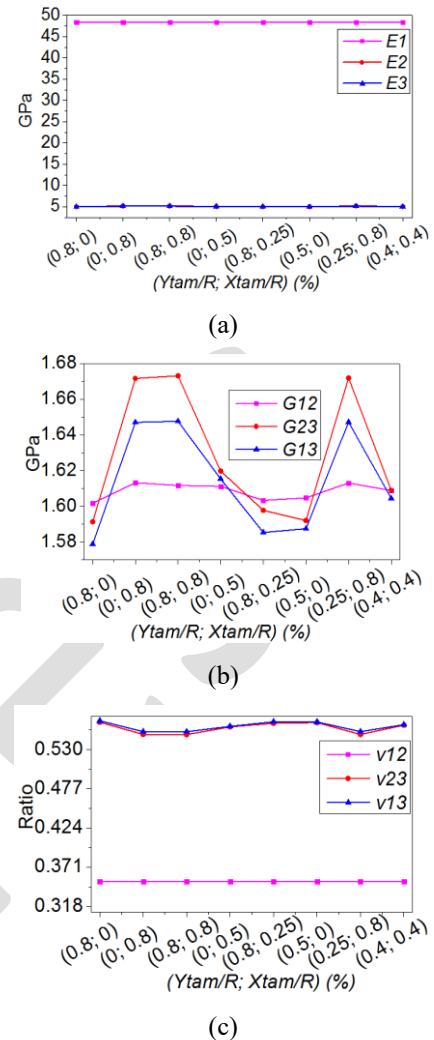


Fig. 8. Influence of fiber eccentricity on the elastic behavior of composite materials

4.3. Effect of Fiber Rotation Angle

In this case we will build a model for the case bkn/bkl equal 0.85 and the rotation angle will change from 0° ; 30° ; 60° ; 90° ; 120° and 150° . Fig. 9 present the relationship between mechanical properties and fiber rotation. To facilitate the calculation of the fiber volume fraction V_f , in this example V_f is set to 0.2, and $Y_{tam}/R = X_{tam}/R = 0.8$. The rotation angle is then applied to the fiber located at the center of the RVE, and the resulting mechanical behavior is evaluated for both hexagonal and square RVE configurations. The same procedure is repeated for fibers located at other positions.

The results indicate that the longitudinal modulus E_1 remains relatively stable, while other mechanical components exhibit irregular variations with increasing fiber rotation angle. These findings suggest that eccentric fiber positioning and cross-sectional

deformation introduce stress states comparable to those observed in random fiber distributions during actual manufacturing. Consequently, when fibers deviate from the RVE center, the effective micro-scale mechanical properties vary unpredictably, making them difficult to capture using conventional theoretical approaches.

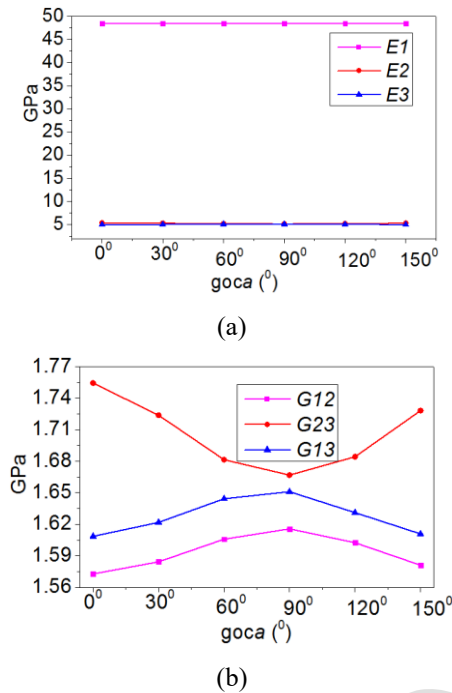


Fig. 9. Effects of fiber rotation angle change on the mechanical properties of T300

4.4. A New Develop Quick Tool Model

To facilitate rapid prediction of effective mechanical properties at the micro-scale, a new intuitive analytical tool was developed based on FEA results obtained from the Python-based application introduced in Section 2. This tool was evaluated against classical analytical models, including Halpin-Tsai, Chamis, and Hashin-Rosen [24], as well as the FEA-based algorithm previously developed. By utilizing optimization techniques and FEA-generated data, the proposed tool enables fast and accurate estimation of micro-scale properties without the computational cost of full FEA simulations. The tool interface is shown in Fig. 10. This approach offers high practical value, allowing designers to efficiently evaluate and optimize the mechanical performance of complex composite materials during the early design stages.

A comparison was conducted between results from analytical models, the FEA-based algorithm developed in Section 2, and the proposed quick prediction tool. The results demonstrate that all methods yield good agreement with FEA results for key properties, including E_1 , E_2 , E_3 , and ν_{12} . However, the prediction accuracy for the shear modulus and ν_{23} remains limited.

Overall, the proposed quick analysis tool enables efficient and reliable prediction of micro-scale RVE properties, closely aligning with the detailed FEA approach while significantly reducing computation time. The validation results for the T300/Epoxy composite using the quick tool, compared with FEA and analytical models, are shown in Fig. 11.

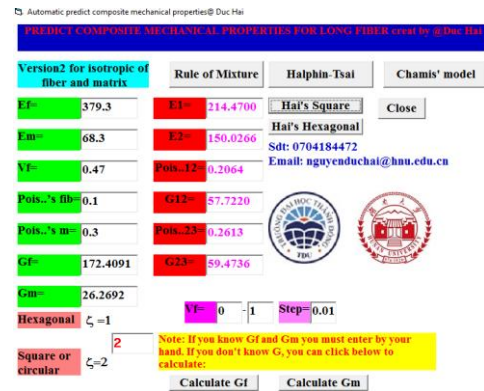


Fig. 10. The interface quick tool for predicting micro-scale RVE

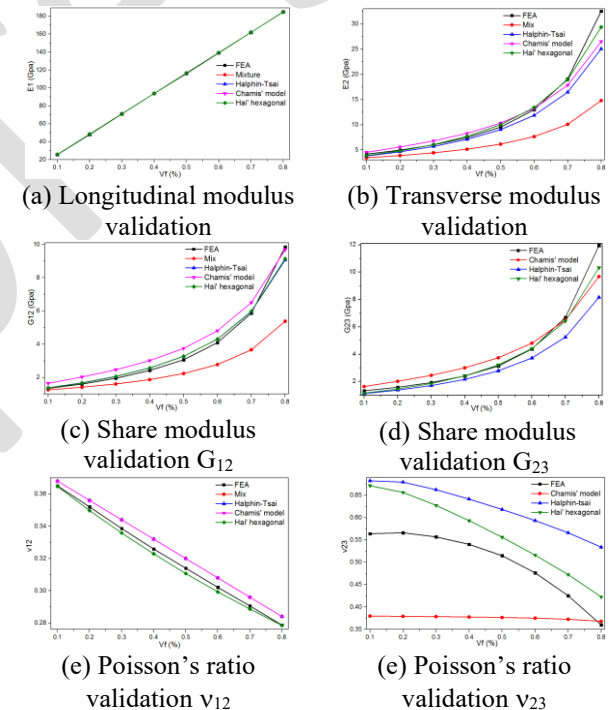


Fig. 11. Results of T300/Epoxy hexagonal RVE using quick tool, FEA with other model

Compared to existing homogenization approaches such as Chamis [15] and Halpin-Tsai [24], the proposed model shows higher sensitivity to microstructural randomness, particularly in predicting shear modulus and Poisson's ratios. This is consistent with recent studies by Liu *et al.* [5] and Chang *et al.* [8, 9], which also emphasized the importance of capturing fiber eccentricity and matrix deformation in

micro-scale analysis. Our results confirm and extend these findings by offering a practical tool for modeling such effects efficiently.

5. Conclusion

This paper presents a Python-based, open-source tool integrated with Abaqus CAE for efficient modeling and homogenization of 3D FRP composites at the micro-scale. The tool enables automated generation of RVEs, application of PBCs, and direct extraction of elastic constants, supporting both idealized and manufacturing-informed microstructures. The extended analysis demonstrated that fiber eccentricity, shape irregularities, and rotational misalignments significantly influence transverse moduli and Poisson's ratios, while longitudinal stiffness remains relatively stable. Comparison with experimental and numerical results from the literature confirmed the accuracy and flexibility of the proposed approach. The ability to simulate non-ideal geometries offers a practical advantage over traditional models, which often assume perfect fiber alignment and periodicity.

Key contributions include:

- (1) An intuitive and customizable graphical interface for rapid RVE creation and property evaluation.
- (2) Integration of stochastic effects such as fiber shape and position randomness into the FE-RVE workflow.
- (3) A validated quick prediction module for estimating micro-scale elastic constants without requiring full FEA.

This tool provides a useful foundation for multi-scale design, material screening, and optimization of FRP composites in structural applications. Future work will focus on extending the model to account for nonlinear behavior, thermal effects, and damage evolution to better reflect complex service conditions in real-world composite structures.

Funding Declaration

The authors declare that no funding was received to support this study.

Author Contributions:

Nguyen Duc Hai contributed to the development of the computational framework, implementation of the Python-Abaqus interface, finite element modeling, data analysis, and manuscript writing.

References

- [1] S. -S. Yao, F. L. Jin, K. Y. Rhee, D. Hui, and S. -J. Park, Recent advances in carbon-fiber-reinforced thermoplastic composites: A review, *Composites Part B: Engineering*, vol. 142, pp. 241–250, Jun. 2018. <https://doi.org/10.1016/j.compositesb.2017.12.007>
- [2] W. Tian, L. Qi, J. Zhou, J. Liang, and Y. Ma, Representative volume element for composites reinforced by spatially randomly distributed discontinuous fibers and its applications, *Composite Structures*, vol. 131, pp. 366–373, Nov. 2015. <https://doi.org/10.1016/j.compstruct.2015.05.014>
- [3] N. Li and Y. D. Zhou, Failure mechanism analysis of fiber-reinforced polymer composites based on multi-scale fracture plane angles, *Thin-Walled Structures*, vol. 158, Jan. 2021, Art. no. 107195. <https://doi.org/10.1016/j.tws.2020.107195>
- [4] Y. Chu, L. Sun, X. Yang, J. Wang, and W. Huang, Multiscale simulation and theoretical prediction for the elastic properties of unidirectional fiber - reinforced polymer containing random void defects, *Polymer Composites*, vol. 42, iss. 6, pp. 2958–2972, Mar. 2021. <https://doi.org/10.1002/pc.26028>
- [5] P. F. Liu and X. K. Li, Explicit finite element analysis of failure behaviors of thermoplastic composites under transverse tension and shear, *Composite Structures*, vol. 192, pp. 131–142, May 2018. <https://doi.org/10.1016/j.compstruct.2018.02.037>
- [6] K. Raju, T-E. Tay, and V. B. C. Tan, A review of the FE² method for composites, *Multiscale and Multidisciplinary Modeling, Experiments and Design*, vol. 4, pp. 1–24, Jan. 2021. <https://doi.org/10.1007/s41939-020-00087-x>
- [7] Q. Guo, W. Yao, W. Li, N. Gupta, Constitutive models for the structural analysis of composite materials for the finite element analysis: A review of recent practices, *Composite Structures*, vol. 260, Mar. 2021, Art. no. 113267. <https://doi.org/10.1016/j.compstruct.2020.113267>
- [8] C. Chang, Y. Zhang, and H. Wang, Micromechanical modeling of unidirectional composites with random fiber and interphase thickness distributions, *Archive of Applied Mechanics*, vol. 89, iss. 12, pp. 2563–2575, Dec. 2019. <https://doi.org/10.1007/s00419-019-01595-0>
- [9] H. Bisheh, Automatic generation of 3D micromechanical finite element model with periodic boundary conditions to predict elastic properties of bamboo fibre-reinforced composites, *Structures*, vol. 58, Dec. 2023, Art. no. 105639. <https://doi.org/10.1016/j.istruc.2023.105639>
- [10] C. Cai, B. Wang, W. Yin, Z. Xu, R. Wang, and X. He, A new algorithm to generate non-uniformly dispersed representative volume elements of composite materials with high volume fractions, *Materials & Design*, vol. 219, Jul. 2022, Art. no. 110750. <https://doi.org/10.1016/j.matdes.2022.110750>
- [11] W. Wang, H. Wang, S. Fei, H. Wang, H. Dong, and Y. Ke, Generation of random fiber distributions in fiber reinforced composites based on Delaunay triangulation, *Materials & Design*, vol. 206, Aug. 2021, Art. no. 109812. <https://doi.org/10.1016/j.matdes.2021.109812>
- [12] T. J. Vaughan and C. T. McCarthy, A combined experimental–numerical approach for generating

- statistically equivalent fibre distributions for high strength laminated composite materials, *Composites Science and Technology*, vol. 70, iss. 2, pp. 291–297, Feb. 2010.
<https://doi.org/10.1016/j.compscitech.2009.10.020>
- [13] K. Naresh, K. A. Khan, R. Umer, and W.-J. Cantwell, The use of X-ray computed tomography for design and process modeling of aerospace composites: A review, *Materials & Design*, vol. 190, May 2020, Art. no. 108553.
<https://doi.org/10.1016/j.matdes.2020.108553>
- [14] W. Tian, L. Qi, X. Chao, J. Liang, and M. Fu, Periodic boundary condition and its numerical implementation algorithm for the evaluation of effective mechanical properties of the composites with complicated micro-structures, *Composites Part B: Engineering*, vol. 162, pp. 1–10, Apr. 2019.
<https://doi.org/10.1016/j.compositesb.2018.10.053>
- [15] F. Otero, S. Oller, X. Martínez, O. Salomón, Numerical homogenization for composite materials analysis. Comparison with other micro mechanical formulations, *Composite Structures*, vol. 122, pp. 405–416, Apr. 2015.
<https://doi.org/10.1016/j.compstruct.2014.11.041>
- [16] X. -Y. Zhou, P. D. Gosling, Z. Ullah, and Ł. Kaczmarczyk, Exploiting the benefits of multi-scale analysis in reliability analysis for composite structures, *Composite Structures*, vol. 155, pp. 197–212, Nov. 2016.
<https://doi.org/10.1016/j.compstruct.2016.08.015>
- [17] V. D. Nguyen, E. Béchet, C. Geuzaine, and L. Noels, Imposing periodic boundary condition on arbitrary meshes by polynomial interpolation, *Computational Materials Science*, vol. 55, pp. 390–406, Apr. 2012.
<https://doi.org/10.1016/j.commatsci.2011.10.017>
- [18] S. Bargmann, B. Klusemann, J. Markmann, J. E. Schnabel, K. Schneider, C. Soyarslan, and J. Wilmer, Generation of 3D representative volume elements for heterogeneous materials: A review, *Progress in Materials Science*, vol. 96, pp. 322–384, Jul. 2018.
<https://doi.org/10.1016/j.pmatsci.2018.02.003>
- [19] Y. Lai, Y. J. Zhang, L. Liu, X. Wei, E. Fang, and J. Lua, Integrating CAD with Abaqus: A practical isogeometric analysis software platform for industrial applications, *Computers & Mathematics with Applications*, vol. 74, iss. 7, pp. 1648–1660, Oct. 2017.
<https://doi.org/10.1016/j.camwa.2017.03.032>
- [20] S. M. Kastuar, C. E. Ekuma, and Z. -L. Liu, Efficient prediction of temperature-dependent elastic and mechanical properties of 2D materials, *Scientific Reports*, vol. 12, Mar. 2022, Art. no. 3776.
<https://doi.org/10.1038/s41598-022-07819-8>
- [21] E. J. Barbero, T. M. Damiani, and J. Trovillion, Micromechanics of fabric reinforced composites with periodic microstructure, *International Journal of Solids and Structures*, vol. 42, iss. 9–10, pp. 2489–2504, May 2005.
<https://doi.org/10.1016/j.ijsolstr.2004.09.034>
- [22] F. Ye and H. Wang, A simple Python code for computing effective properties of 2D and 3D representative volume element under periodic boundary conditions, *Computational Engineering, Finance, and Science*, Mar. 2017.
<https://doi.org/10.48550/arXiv.1703.03930>
- [23] B. R. Hill, Elastic properties of reinforced solids: Some theoretical principles, *Journal of the Mechanics and Physics of Solids*, vol. 11, iss. 5, pp. 357–372, Sep. 1963.
[https://doi.org/10.1016/0022-5096\(63\)90036-X](https://doi.org/10.1016/0022-5096(63)90036-X)
- [24] R. Younes, A. Hallal, F. Fardoun, and F. H. Chehade, Comparative review study on elastic properties modeling for unidirectional composite materials, *Composites and Their Properties*, Aug. 2012.
<https://doi.org/10.5772/50362>